



Alternative Optics Design: Nonlinear Collimation System

A. Faus-Golfe*, D. Schulte, F Zimmermann,† J. Resta-Lopez‡ T. Asaka§

March 27, 2006

Abstract

The collimation system of a Linear Collider must serve multiple purposes and fulfill a number of constraints. In particular, we require that the collimation system should sustain the impact of off-energy bunches and have a large chromatic bandwidth, in addition to ensuring a high collimation efficiency and tolerable wake fields. We describe the design of a nonlinear energy collimation system for CLIC at 3 TeV, in which skew sextupoles are used to blow up the vertical beam size at the spoiler, so as to guarantee collimator survival in case of beam impact. Its properties, like chromatic bandwidth and collimation survival, are evaluated and compared with those of the baseline linear collimation system.

*IFIC-Valencia, Spain

†CERN, Geneva, Switzerland

‡CERN/IFIC

§CERN/SPring-8

1 Introduction

The collimation system of a Linear Collider (LC) should (1) reduce the background in the detector by removing particles at large betatron amplitudes or energy offsets, which otherwise would be lost generating muons near the Interaction Point (IP) or emit synchrotron radiation (SR) photons in the final doublet; (2) withstand the impact of a full bunch train in case of machine failure, and (3) not produce intolerable wake fields that might degrade the orbit stability or dilute the emittance.

The basic layout of a nonlinear collimation system is illustrated in Fig. 1. The purpose of the first nonlinear element is to blow up beam sizes and particle amplitudes, so that the collimator jaw can be placed further away from the nominal beam orbit (reducing the wake fields) and the beam density is decreased (for collimator survival). A second nonlinear element downstream of the spoiler, and π from the first nonlinear element, cancels all aberrations induced by the former.

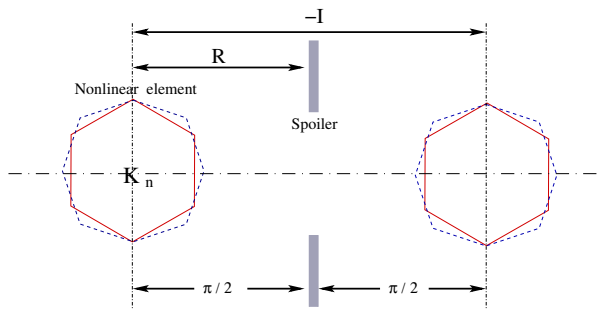


Figure 1: Schematic of a nonlinear collimation system.

At each nonlinear element a particle suffers deflections $\Delta q'_i = -\partial H_n / \partial q_i$, where H_n is the Hamiltonian of the multipole. As was pointed in Ref. [1], higher-order multipoles (decapoles, dodecapoles, etc.) are not useful, because they do not penetrate to the small distances necessary. Skew sextupoles and octupoles could be used.

Different types of nonlinear collimation systems for future linear colliders have been described in the literature [1, 2, 3, 4]:

- For the NLC, in [1] a scheme with skew-sextupole pairs for nonlinear betatron collimation in the vertical plane has been proposed.
- Subsequently, in [2], a halo reduction method with the addition of “tail-folding” octupoles (‘Chebyshev arrangement of octupoles’) in the NLC final focus system is presented (see also [5] for an earlier study with only 1 octupole in front of the final doublet).
- For the TESLA post-linac collimation system a magnetic energy spoiler (MES) has been suggested [3]. An octupole is placed at a high dispersion point between a pair of skew sextupoles (at $\pi/2$ phase advance from the octupole). The skew

sextupoles are separated by an optical transfer matrix $-I$. The result is a significant increase in the vertical beam size at a downstream momentum spoiler.

A characteristic feature of all these systems is that they separate between energy and betatron collimation, and typically employ the nonlinear elements only in one or the other half.

A nonlinear collimation system for CLIC with three skew sextupoles was explored in [4]. It contains a single vertical spoiler which collimates in the horizontal and vertical betatron amplitude at both betatron phases as well as in energy. The scheme is illustrated in Fig. 2. More details of this system can be found in Ref. [4].

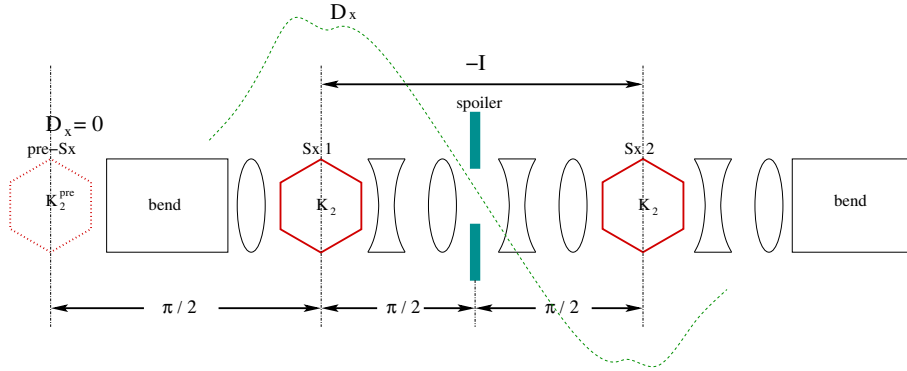


Figure 2: Schematic of a nonlinear collimation system for CLIC [4].

2 Nonlinear Energy Collimation for Linear Colliders using pair of skew sextupoles

In this section we describe a nonlinear energy collimation system based on the layout of [4]. We have refined the equations describing the energy collimation for two different beam momentum distributions.

The integrated sextupole strength K_s can be expressed in terms of the sextupole length l_s , the pole-tip field B_T , the magnetic rigidity $(B\rho)$, and sextupole aperture a_s as

$$K_s = \frac{2B_T l_s}{(B\rho) a_s^2}. \quad (1)$$

The sextupole at a location with horizontal dispersion $D_{x,\text{sext}}$ deflects a passing particle by

$$\Delta x' = K_s (D_{x,\text{sext}} \delta + x) y, \quad (2)$$

$$\Delta y' = -\frac{1}{2} K_s (y^2 - x^2 - D_{x,\text{sext}}^2 \delta^2 - 2D_{x,\text{sext}} \delta x), \quad (3)$$

with δ the relative momentum offset.

The position at the downstream spoiler is obtained from

$$x_{\text{sp}} = x_{0,\text{sp}} + R_{12}\Delta x' , \quad (4)$$

$$y_{\text{sp}} = y_{0,\text{sp}} + R_{34}\Delta y' , \quad (5)$$

where $x_{0,\text{sp}} = x_{\beta,\text{sp}} + D_{x,\text{sp}}\delta$ and $y_{0,\text{sp}} = y_{\beta,\text{sp}}$ are the horizontal and vertical position of the particle at the spoiler without the sextupole, written in terms of the betatronic parts, $x_{\beta,\text{sp}}$ and $y_{\beta,\text{sp}}$, and the horizontal dispersion at the spoiler, $D_{x,\text{sp}}$. For flat beams, such as in the case of CLIC, $x_{\beta} \gg y_{\beta}$. R_{12} and R_{34} at the optical transport matrix elements between the skew sextupole and the spoiler.

The transversal root mean squared beam sizes at the spoiler are given by the expressions

$$\sigma_x = \sqrt{\langle x_{\text{sp}}^2 \rangle - \langle x_{\text{sp}} \rangle^2} , \quad (6)$$

$$\sigma_y = \sqrt{\langle y_{\text{sp}}^2 \rangle - \langle y_{\text{sp}} \rangle^2} . \quad (7)$$

The horizontal mean squared position of particles at the spoiler is given by

$$\begin{aligned} \langle x_{\text{sp}}^2 \rangle &= \langle (x_{\beta,\text{sp}} + D_{x,\text{sp}}\delta + R_{12}K_s(D_{x,\text{sext}}\delta + x_{\beta,\text{sext}})y_{\beta,\text{sext}})^2 \rangle \\ &\simeq \langle (D_{x,\text{sp}}\delta + R_{12}K_s D_{x,\text{sext}}\delta y_{\beta,\text{sext}})^2 \rangle , \end{aligned} \quad (8)$$

and the average horizontal beam offset by

$$\langle x_{\text{sp}} \rangle = D_{x,\text{sp}}\langle \delta \rangle . \quad (9)$$

In the approximation we assume that x_{β} and y_{β} are small compared with $D_x\delta$ both at the spoiler and at the sextupole.

In a similar way, the vertical mean squared position at the spoiler is

$$\begin{aligned} \langle y_{\text{sp}}^2 \rangle &= \langle (y_{\beta,\text{sp}} - \frac{1}{2}R_{34}K_s(y_{\beta,\text{sp}}^2 - x_{\beta,\text{sp}}^2 - D_{x,\text{sext}}^2\delta^2 - 2D_{x,\text{sext}}\delta x_{\beta,\text{sext}}))^2 \rangle \\ &\simeq \frac{1}{4}R_{34}^2 K_s^2 D_{x,\text{sext}}^4 \langle \delta^4 \rangle , \end{aligned} \quad (10)$$

and the average vertical offset

$$\begin{aligned} \langle y_{\text{sp}} \rangle &= \langle (y_{\beta,\text{sp}} - \frac{1}{2}R_{34}K_s(y_{\beta,\text{sp}}^2 - x_{\beta,\text{sp}}^2 - D_{x,\text{sext}}^2\delta^2 - 2D_{x,\text{sext}}\delta x_{\beta,\text{sext}})) \rangle \\ &\simeq \frac{1}{2}R_{34}K_s D_{x,\text{sext}}^2 \langle \delta^2 \rangle . \end{aligned} \quad (11)$$

From Eqs. (6), (7), (8), (9), (10) and (11), considering a *Gaussian momentum distribution*:

$$P(\delta) = \frac{1}{\sqrt{2\pi}\sigma_{\delta}} e^{-1/2\left(\frac{\delta+\delta_0}{\sigma_{\delta}}\right)^2} , \quad (12)$$

with a width σ_δ and with an average momentum offset δ_0 , the transverse beam sizes at the spoiler take the form:

$$\sigma_x \simeq \left(D_{x,\text{sp}}^2 \sigma_\delta^2 + R_{12}^2 K_s^2 D_{x,\text{sext}}^2 (\delta_0^2 + \sigma_\delta^2) \beta_{y,\text{sext}} \epsilon_y \right)^{1/2}, \quad (13)$$

$$\sigma_y \simeq \left(\frac{1}{2} R_{34}^2 K_s^2 D_{x,\text{sext}}^4 (\sigma_\delta^4 + 2\delta_0^2 \sigma_\delta^2) \right)^{1/2}. \quad (14)$$

On the other hand, if we consider the case of a *uniform flat momentum distribution*:

$$P(\delta) = \begin{cases} 0 & \text{for } \delta < -\frac{\delta_{\text{flat}}}{2} + \delta_0 \\ \frac{1}{\delta_{\text{flat}}} & \text{for } -\frac{\delta_{\text{flat}}}{2} + \delta_0 < \delta < \frac{\delta_{\text{flat}}}{2} + \delta_0 \\ 0 & \text{for } \delta > \frac{\delta_{\text{flat}}}{2} + \delta_0, \end{cases} \quad (15)$$

with a full width δ_{flat} and an average momentum offset δ_0 , the transverse beam sizes at the spoiler take the form:

$$\sigma_x \simeq \left(D_{x,\text{sp}}^2 \frac{\delta_{\text{flat}}^2}{12} + R_{12}^2 K_s^2 D_{x,\text{sext}}^2 \left(\frac{\delta_{\text{flat}}^2}{12} + \delta_0^2 \right) \beta_{y,\text{sext}} \epsilon_y \right)^{1/2}, \quad (16)$$

$$\sigma_y \simeq \left(\frac{1}{4} R_{34}^2 K_s^2 D_{x,\text{sext}}^4 \left(\frac{\delta_{\text{flat}}^4}{180} + \frac{1}{3} \delta_{\text{flat}}^2 \delta_0^2 \right) \right)^{1/2}. \quad (17)$$

For spoiler survival, a minimum beam size $\sigma_{r,\text{min}}$ is required so that $\sigma_y \sigma_x \geq \sigma_{r,\text{min}}^2$.

We can perform the energy collimation with a vertical or horizontal spoiler, using either the nonlinear second order vertical dispersion or the linear horizontal dispersion at the location of the spoiler. Alternatively, we can also use a spoiler for both planes with properly chosen horizontal and vertical gap sizes, so that the collimation occurs at the same momentum offset in the two planes.

If we employ a vertical spoiler, the nonlinear terms in the sextupolar deflection also yields a weak collimation for horizontal or vertical betatron amplitudes, at a collimation depth in units of σ_x or σ_y respectively of

$$n_x = \frac{D_{x,\text{sext}} \Delta}{\sqrt{\epsilon_x \beta_{x,\text{sext}}}}, \quad (18)$$

$$n_y = \frac{D_{x,\text{sext}} \Delta}{\sqrt{\epsilon_y \beta_{y,\text{sext}}}}, \quad (19)$$

where Δ is the energy collimation depth in units of δ . We can solve these equations for the beta functions at the sextupole and match for meaningful values of n_x and n_y . This was the approach chosen in [4], which tended to introduce large chromaticity.

Additionally, we can collimate in the other betatron phase, using the linear optics. Denoting the horizontal and vertical spoiler half gaps by a_x and a_y , respectively, and assuming that the vertical gap is adjusted for collimation at the same offset Δ as the

horizontal one, instead of (18) and (19) we would get (dependent on the plane of linear collimation)

$$n_x^{(2)} = \frac{a_x}{\sqrt{\epsilon_x \beta_{x,\text{sp}}}} \simeq \frac{D_{x,\text{sp}} \Delta}{\sqrt{\epsilon_x \beta_{x,\text{sp}}}}, \quad (20)$$

$$n_y^{(2)} = \frac{a_y}{\sqrt{\epsilon_y \beta_{y,\text{sp}}}} \simeq \frac{1}{2} \frac{|R_{34} K_s| D_{x,\text{sp}}^2 \Delta^2}{\sqrt{\epsilon_y \beta_{y,\text{sp}}}}, \quad (21)$$

where a_x and a_y are the half gap at the spoiler, and the super-index (2) refers to the orthogonal betatron phase, considering that the spoiler and the skew sextupole are placed roughly 90 degrees out of phase. These equations can be matched for the beta functions at the spoiler.

In principle, by combining Eqs. (18), (19), (20) and (21), we could collimate in both betatron phases and in energy using a single spoiler. If we opt for nonlinear betatron collimation, the other phase could also be collimated by installing a “pre” skew sextupole with a phase advance of about $\pi/2$ in front of the first skew sextupole, as proposed in [4].

The achievable value of the dispersion $D_{x,\text{sext}}$ is limited by the emittance growth $\Delta(\gamma\epsilon_x)$ due to synchrotron radiation in the dipole magnets. The latter restricts the value

$$\Delta(\gamma\epsilon_x) \approx (4 \times 10^{-8} \text{ m}^2 \text{ GeV}^{-6}) E^6 I_5 < f \epsilon_x \quad (22)$$

to a fraction f of the initial emittance. Here I_5 is the radiation integral [6], $I_5 = \sum_i L_i < \mathcal{H} > / |\rho_i|^3$, the sum runs over all bending magnets, with bending radius ρ_i , length L_i , and the “curly \mathcal{H} ” function as defined by Sands [7].

3 Non Linear Energy Collimation system for CLIC using pair of skew Sextupoles

3.1 Optics Design

Two new optics designs for nonlinear energy collimation at CLIC were developed and optimized. The main changes with respect to the previous nonlinear collimation optics [4] are:

- The collimation is performed only in energy. The sole purpose of the first skew sextupole is to increase vertical spot size at the spoiler. A horizontal spoiler and the linear horizontal optics are used for the energy collimation.
- We have increased the overall fraction of the system occupied by bends and decreased the bending angle until the effect of synchrotron radiation became reasonably small.
- We kept the beta functions as regular as possible to avoid need of a dedicated chromatic correction inside the collimation system.

One of the two new optics features no dipoles between the two main skew sextupoles, the other has a high filling factor of dipole magnets. Both optics are displayed in Fig.3.

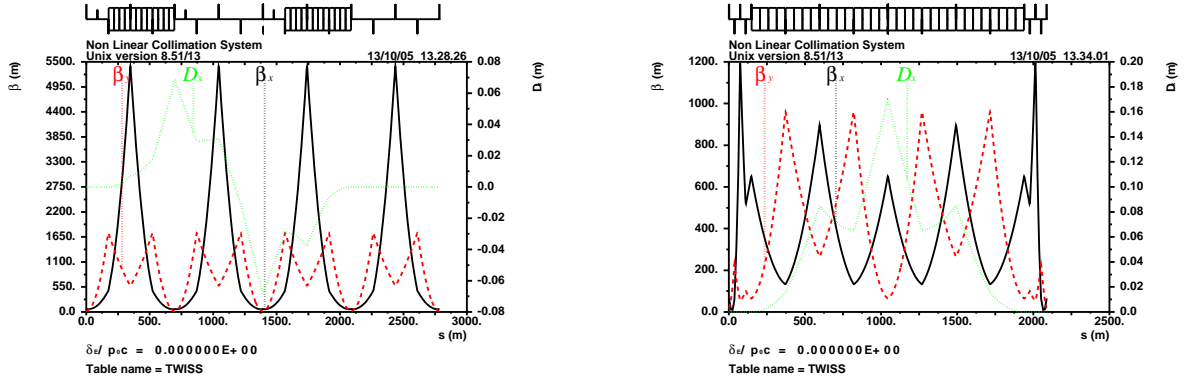


Figure 3: Optics of the new nonlinear energy collimation system without (left) and with bends between the skew sextupoles (right).

The beta functions are kept approximately constant along the line, which results in negligible chromatic emittance growth. The dispersion at the first main skew sextupole and the skew-sextupole strength are chosen so as to guarantee spoiler survival in case of a full beam impact. Notice that in the case with high filling factor of dipole magnets there is no change of sign in the dispersion function. The length of the two systems was reduced to the minimum value for which emittance growth due to synchrotron radiation does not yet affect the collider performance. The bending angles were adjusted accordingly. Beam, collimation and optics parameters of CLIC at 3 TeV are listed in Table 1 for the two optics. In the calculation of the collimation and beam parameters we have considered a *uniform flat momentum distribution*. The minimum beam size required for spoiler survival is about $\sigma_{r,\min} \approx 120 \mu\text{m}$ (allowing for carbon or beryllium as spoiler material) [8]. A value of $I_5 = 10^{-19} \text{ m}$ corresponds to $\Delta(\gamma\epsilon_x) \approx 0.046 \mu\text{m}$ for CLIC at 3 TeV or to about 7% emittance growth, but chromatic effects may further increase the luminosity degradation due to synchrotron radiation. The value $I_5 = 10^{-19} \text{ m}$ has been taken as constraint for the dispersion function and dipole angle in the optics design.

3.2 Tracking studies

Multiparticle tracking studies were done using an initial distribution of 10000 particles with 1% full width energy spread for a flat square energy distribution, δ_{flat} . Different average energy offsets δ_0 for such a particle distribution were further considered. The tracking along the two optical systems of Fig. 3, from the entrance to the spoiler location, was done using the code MAD [9]. The simulated horizontal and vertical rms beam sizes at the spoiler were calculated from the tracking result as a function of the skew sextupole strength and δ_0 , and compared with the analytical expressions (16) and (17), which represent a first order calculation). A good agreement was obtained for the vertical

Table 1: Beam, optics and collimation parameters for the two new nonlinear energy collimation systems without and with bends between the skew sextupoles.

variable	symbol	w/o bends	w bends	units
beam energy	E	1.5	1.5	TeV
rms momentum spread	σ_ϵ	2.8×10^{-3}	2.8×10^{-3}	
hor. geom. emittance	ϵ_x	0.23	0.23	pm
vert. geom. emittance	ϵ_y	6.8	6.8	fm
full width	δ_{flat}	0.01	0.01	
total length	l_t	2784.0	2088.0	m
cell length	l_c	170.0	220.0	m
dipole angle	θ_b	0.00008	0.00014	rad
skew sextupole pole tip field	B_T	1.4	1.4	T
skew sextupole aperture	a_s	4	4	mm
skew sextupole length	l_s	3	3	m
skew sextupole strength	K_s	104.3	104.3	m^{-2}
hor. beta function at entrance	β_x^0	65.0	650.0	m
ver. beta function at entrance	β_y^0	18.0	65.0	m
hor. phase advance from sext. to spo.	μ_x	0.322	0.250	2π
ver. phase advance from sext. to spo.	μ_y	0.293	0.500	2π
transport matrix from sext. to spo.	R_{12}	86.6	763.2	m
transport matrix from sext. to spo.	R_{34}	87.4	131.5	m
hor. dispersion function at sext.	$D_{x,\text{sext}}$	0.049	0.085	m
hor. dispersion function at spo.	$D_{x,\text{sp}}$	-0.068	0.170	m
synchrotron integral	I_5	2.9×10^{-21}	1.0×10^{-20}	m
spoiler survival size	$\sigma_{r,\text{sp}}$	126.4	424.7	μm
energy collimation depth	Δ	0.013	0.013	
hor. spoiler half gap	$a_{x,\text{sp}}$	0.089	2.206	mm
ver. spoiler half gap	$a_{y,\text{sp}}$	1.835	8.343	mm

case, as is illustrated in Figs. 4 and 5 (left pictures). However, an analytical description including second and third order transport coefficients is necessary to reproduce the trend of the simulations for the horizontal case, shown in the right pictures of Figs. 4 and 5.

For the optics solution of Fig. 3 (left), the horizontal rms beam size decreases for values $\delta_0 < 2.5\%$ (see right picture of Fig. 4). For higher average energy offsets, the horizontal beam size increases steeply. Figure 6 (right picture) illustrates how the horizontal particle distribution with $\delta_0 = 1\%$ shrinks at the spoiler position due to the effect of the skew sextupole. On the other hand, for the optics solution of Fig. 3 (right), the horizontal rms beam size increases smoothly as a function of δ_0 ; see Figs. 5 and 7. This behavior is desired to increase the probability of spoiler survival.

In order to study the luminosity performance of the two optics solutions for nonlinear

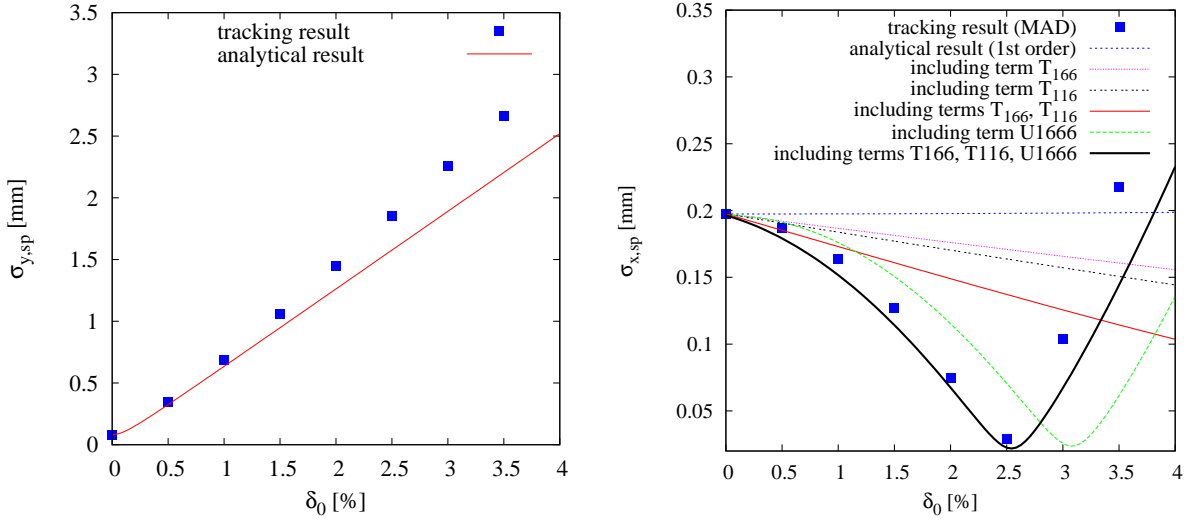


Figure 4: Vertical (left) and horizontal rms beam size (right) as a function of the average energy offset δ_0 , for the optics solution of Fig. 3 (left).

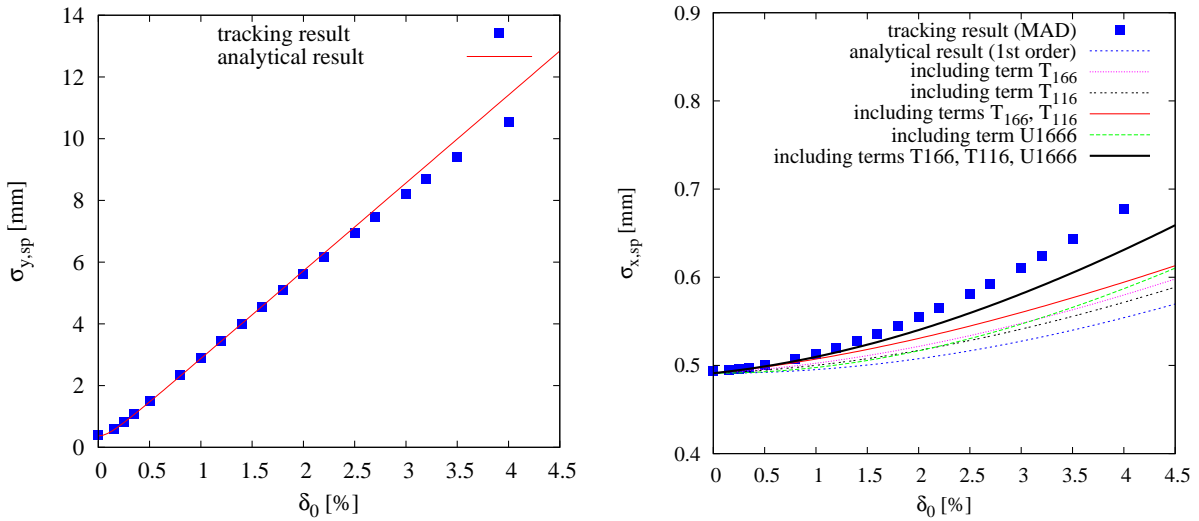


Figure 5: Vertical (left) and horizontal rms beam size (right) as a function of the average energy offset δ_0 , for the optics solution of Fig. 3 (right).

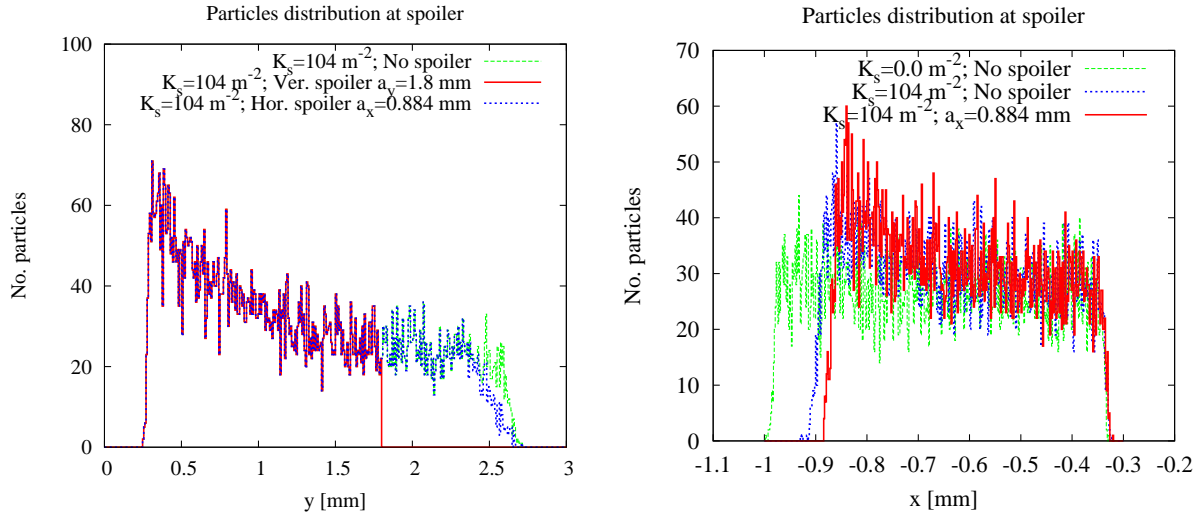


Figure 6: Vertical (left) and horizontal particle distribution (right) with an average energy offset of 1% at the spoiler, for the optics solution of Fig. 3 (left), considering various skew-sextupole strengths and collimator settings.

collimation, we tracked a distribution of 40000 particles with 1% full width energy spread from the entrance of the collimation system to the interaction point. The corresponding optics are displayed in Figs. 8. The cases with and without synchrotron radiation have been considered in these simulations. The luminosity has been computed by the beam-beam interaction code **GUINEA-PIG** [10]. This program performs detailed simulations of the beam-beam interactions at the IP, including the hourglass effect, the pinch effect, beamstrahlung and e^+e^- production. In Fig. 9 we present the simulated luminosity as a function of the skew sextupole strength for the two optics solutions of Fig. 3. The luminosity for either optics drops with the excitation of the skew sextupoles. The decrease for optics without bends between the skew sextupoles is moderate; on the other hand, for the optics with high filling factor of bends between the skew sextupoles the luminosity drops dramatically, losing almost two orders of magnitude for $K_s = 104 \text{ m}^{-2}$ with respect to the value of luminosity for $K_s = 0 \text{ m}^{-2}$. For comparison, the linear baseline CLIC collimation system provides a luminosity of $L_{w/oSR} = 10.714 \times 10^{34} \text{ cm}^{-2}\text{s}^{-1}$ and $L_{wSR} = 7.441 \times 10^{34} \text{ cm}^{-2}\text{s}^{-1}$ calculated using the codes **MAD** [9] and **GUINEA-PIG** [10], from [11].

4 Outlook

Two new optics designs for the CLIC nonlinear energy collimation were developed and optimized, one with a high filling factor of dipole magnets, the other without any dipoles between the two main skew sextupoles. The beta functions are kept approximately constant along the line, which results in negligible chromatic emittance growth. The dispersion at the first main skew sextupole and the skew-sextupole strength are chosen

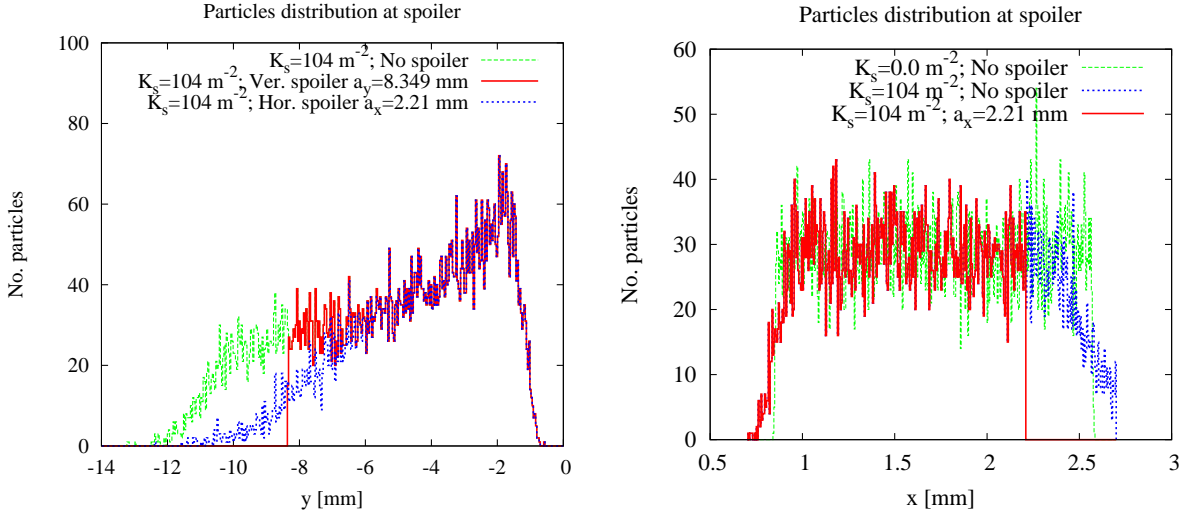


Figure 7: Vertical (left) and horizontal particle distribution (right) with an average energy offset of 1% at the spoiler, for the optics solution of Fig. 3 (right), considering various skew-sextupole strengths and collimator settings.

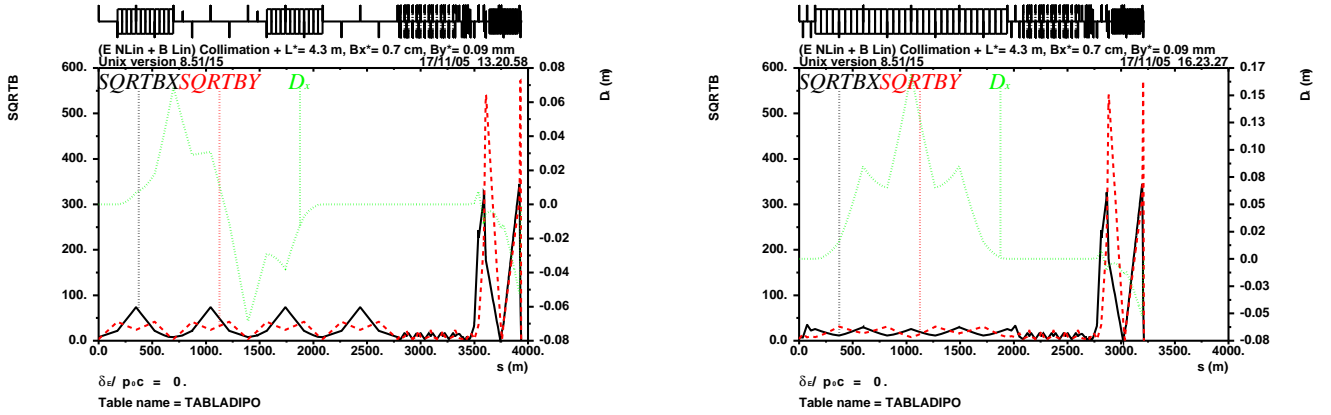


Figure 8: Optics of the complete CLIC beam delivery system with nonlinear energy collimation using a pair of skew sextupoles from Fig. 3. Both optics, without and with bends between the skew sextupoles, were designed using the code MAD.

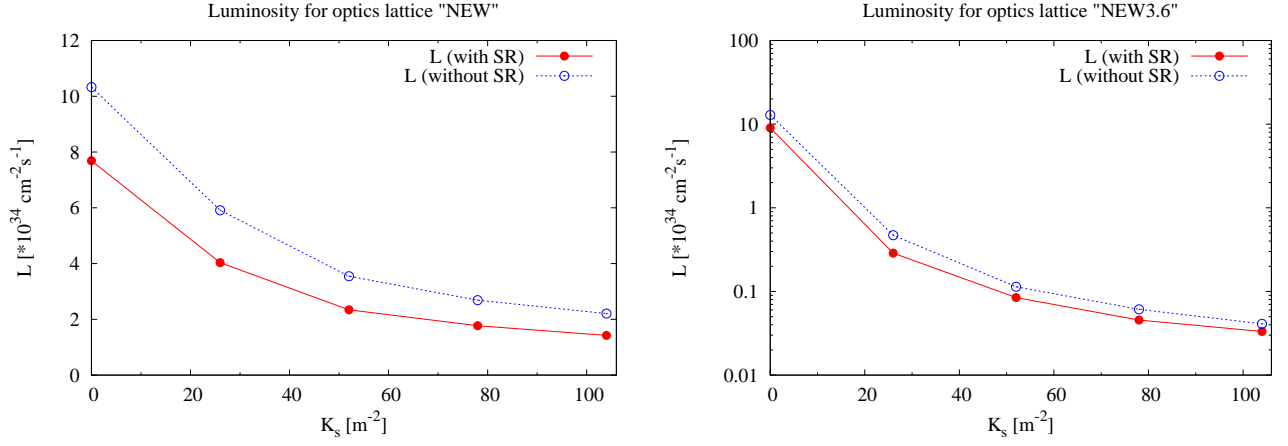


Figure 9: Luminosity as a function of the integrated skew sextupole strength, for the two optics solutions of Figs. 3 or 8. The two curves refer to MAD simulations with and without synchrotron radiation. The luminosity was computed by GUINEA-PIG.

so as to guarantee spoiler survival in case of a full beam impact. The length of the two systems was reduced to the minimum value for which emittance growth due to synchrotron radiation does not yet affect the collider performance. The bending angles were adjusted accordingly.

The chromatic behavior of the optics was characterized, and the simulated horizontal and vertical rms beam sizes at the spoiler as a function of the skew sextupole strength were compared with analytical expressions. A good agreement was obtained after accounting for second and third order expansion coefficients of the optical transport.

For zero skew sextupole strength, the luminosity for both new optics exceeds that of the CLIC baseline linear collimation system. However, the luminosity for either optics drops with the excitation of the skew sextupoles. The better performance is obtained for the optics without any dipoles between the skew sextupoles. It has, therefore, been chosen as a reference for future improvements.

Fortunately, it was realized that the skew sextupole strengths can be set to much lower values than previously assumed, if a maximum beam density for spoiler survival is required only for an off-momentum beam, and not for the nominal one. This is illustrated in Fig. 10. The survival limit corresponds to a density of about $50 \times 10^9 \text{ mm}^{-2}$ per bunch.

Acknowledgement

This work is supported by the Commission of the European Communities under the 6th Framework Programme "Structuring the European Research Area", contract number RIDS-011899.

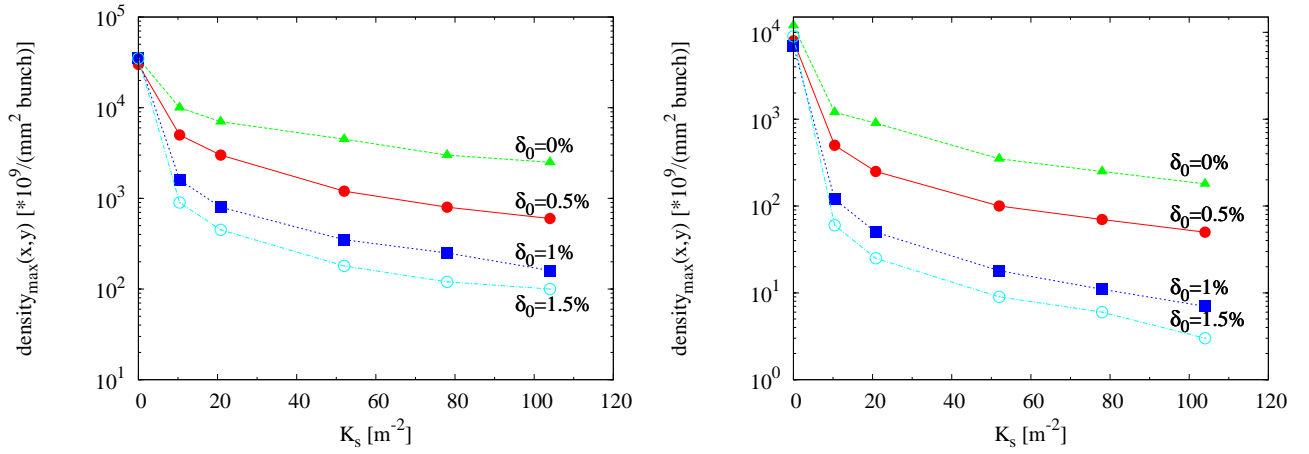


Figure 10: Peak density at the spoiler as a function of the skew sextupole strength for the two optics solutions of Fig. 3.

References

- [1] L. Merminga, J. Irwin, R. H. Helm and R. D. Ruth, "Collimation systems for a TeV linear collider," Part. Accel. 48, 85 (1994) and SLAC-PUB-5165 Rev. may 1994.
- [2] R. Brinkmann, P. Raimondi and A. Seryi, "Halo reduction By Means of Non Linear Optical Elements in the NLC Final Focus System," PAC2001, Chicago (2001).
- [3] R. Brinkmann, N.j. Walker and G. Blair, "The TESLA Post-linac Collimation System," TESLA-01-12 (2001).
- [4] A. Faus-Golfe and F. Zimmermann, "A Nonlinear Collimation System for CLIC," EPAC 2002 Paris (2002).
- [5] K. Thompson, R. Pitthan, F. Zimmermann, et al., NLC Collimation Meetings, in particular 22.05.98, 29.05.98, and 31.08.98.; see web site: http://www-project.slac.stanford.edu/lc/bdir/meetings_collimation.asp
- [6] R. Helm, M. Lee, P. Morton and M. Sands, "Evaluation of Synchrotron Radiation Integrals," SLAC-PUB-1193 (1973).
- [7] M. Sands, "The Physics of Electron Storage Rings," SLAC-121 (1970).
- [8] S. Fartoukh, et al., "Heat Deposition by Transient Beam Passage in Spoilers," CERN-SL-2001-012 AP (2001) and CLIC Note 477.
- [9] H. Grote and F.C. Iselin, "The MAD program (Methodical Accelerator Design) version 8.16," User's reference manual, CERN/SL/90-13(AP) (1995).
- [10] D. Schulte, Ph.D. thesis, University of Hamburg, TESLA-97-08(AP) (1996).

- [11] T. Asaka and J. Resta Lopez, “Characterization and Performance of the CLIC Beam delivery Sysytem with SAD, MAD and Placet”, CARE/ELAN Document 2005-011 (2005).